[Rock and Soil Mechanics](https://rocksoilmech.researchcommons.org/journal)

Volume 42 | Issue 3 Article 5

7-28-2021

Large strain consolidation of sand-drained ground considering the well resistance and the variation of radial permeability coefficient

Wen-hao JIANG

Liang-tong ZHAN
zhanlt@zju.edu.cn

Custom Citation
JIANG Wen-hao, ZHAN Liang-tong. Large strain consolidation of sand-drained ground considering the well resistance and the variation of radial permeability coefficient[J]. Rock and Soil Mechanics, 2021, 42(3): 755-766.

Rock and Soil Mechanics 2021 42(3): 755−766
https: //doi.org/10.16285/j.rsm.2020.6029
ISSN 1000−7598
rocksoilmech.researchcommons.org/journal

Large strain consolidation of sand-drained ground considering the well resistance and the variation of radial permeability coefficient

JIANG Wen-hao, ZHAN Liang-tong
Institute of Geotechnical Engineering, Zhejiang University, Hangzhou, Zhejiang 310058, China

Abstract: Based on Barron's equal strain consolidation theory of sand-drained ground and Gibson's one-dimensional large strain consolidation theory, and considering the well resistance of drains, the variation of radial permeability coefficient and the vertical flow, a more general governing equation of large strain consolidation of sand-drained ground is established and solved by using the finite difference method. The correctness of the numerical solution is verified by comparing with the existing consolidation model and small-strain analytical solution. Using the numerical solution, the large strain consolidation behaviors of sand-drained ground are investigated. The analyses show that the well resistance of drains can reduce the consolidation rate of sand-drained ground. But when the permeability coefficient of drains increases to a certain value, the well resistance of drains can be ignored. The variation pattern of radial permeability coefficient has a great influence on the consolidation rate of sand-drained ground. The consolidation rate is faster under the parabolic pattern than that the linear pattern. The vertical flow accelerates the consolidation rate of sand-drained ground, when the radius ratio is small, and the influence of the vertical flow on the consolidation rate should be considered. The larger the ratio of compression index to permeability index is, the slower the consolidation rate of sand-drained ground will be.

Keywords: sand-drained ground; large strain consolidation; well resistance; radial permeability coefficient; vertical flow; finite difference method

1 Introduction

One of a common method of foundation reinforcement in engineering is by using sand well to treat soft soil foundation, which has been currently widely applied in the construction of airport runway, port, wharf and other projects[1]. Scholars have carried out a large number of theoretical and practical studies on consolidation of sand-drained ground already[2−11]. Based on the hypotheses of equal strain and free strain, Barron[2] has obtained in first, the analytical solution of ideal sand-drained ground. Based on Barron's sand-drained ground consolidation theory, Hansbo et al.[3] have adopted a similar method to solve the consolidation problem of sand-drained ground considering the smear effect and effect of well resistance. Based on the hypothesis of equal strain, Xie et al.[4] have derived and obtained the analytical solution of the radial consolidation of sand-drained ground considering the smear effect and effect of well resistance. By considering the non-linearity consolidation characteristic of the soil, Indraratna et al.[7] have obtained the analytical solution of the non-linear consolidation of sand-drained ground under radial seepage only. Deng et al.[8] have deduced the consolidation solution of sand-drained ground that accords to the change in well resistance with time, by taking the fact of that the permeability coefficient of sand well will decrease gradually in the consolidation process into account. Lu et al.[9] have considered the effect of the well resistance of sand well and studied the non-linear consolidation problem of sand-drained ground under radial and vertical seepages. By considering the variation of radial permeability coefficient, Zhang et al.[11] have analyzed the consolidation problem of sand-drained ground under vacuum preloading. However, all of the studies above are based on the basic hypotheses of small strains and without considering the large strain consolidation characteristic of soil.

In recent years, soft soil foundations with high water content and compressibility are often involved[12−14] in practical projects such as marine and land reclamations. For soft soil foundation with high water content, its settlement is large in the consolidation process, therefore the large strain consolidation theory should be adopted for the studying of it[12−16]. Based on the hypothesis of free strain, Jiang et al.[12] have used the finite difference method to solve the large strain consolidation problem of sand-drained grounds. Zhang et al.[13] have analyzed the large strain consolidation problem of double-layered sand-drained ground by considering the compression−permeability relationship in terms of power function. Based on the large

Received: 18 July 2020 Revised: 29 December 2020
This work was supported by the Key Research and Development Program of Zhejiang Province(2019C03107).
First author: JIANG Wen-hao, male, born in 1996, Postgraduate, majoring in ground treatment. E-mail: 21812025@zju.edu.cn
Corresponding author: ZHAN Liang-tong, male, born in 1972, PhD, Professor, PhD supervisor, research interests: unsaturated soil mechanics, environmental geotechnical engineering and slope engineering. E-mail: zhanlt@zju.edu.cn

strain consolidation theory, Sun et al.[14] have deduced and solved the consolidation problem of unperforated sand-drained ground. Based on the hypothesis of equal strain, Cao et al.[15−16] have established a large strain consolidation model of sand-drained ground with the void ratio as variable, which could consider factors including the effects of smear and vertical seepage on large strain consolidation characteristic of sand-drained ground. By considering the effect of vacuum loads, Indraratna et al.[17] have analyzed the large strain consolidation problem of sand-drained ground under non-Darcy seepage. Based on the semi-logarithmic linear compression−permeability relationship, Geng et al.[18] have studied the large strain consolidation behavior of sand-drained ground by using numerical method. However, the effect of resistance of sand well on the consolidation behavior of sand-drained ground was considered in none of the studies above.

By considering the resistance effect of sand well, Nguyen et al.[19] have analyzed the large strain consolidation behavior of sand-drained ground under equal strain condition. However, when Nguyen et al.[19] considered the effect of resistance of sand well, the average excess pore pressure in sand well was applied for calculation, therefore the solution had a certain similarity. In practical engineering, the radial permeability coefficient of soil gradually changes in coordination with the change in distance from the sand well[20−21], therefore the effect of the variation mode of the radial permeability coefficient on the consolidation behavior of the sand-drained ground should be considered. Additionally, for the consolidation problem of sand-drained ground, ignoring the vertical seepage may significantly underestimate the consolidation rate of sand-drained ground[21] and the effect of vertical seepage on large strain consolidation of sand-drained ground should be considered when considering the integrality of theory of large strain consolidation.

Therefore, based on several large strain consolidation models of sand-drained ground[12−19] listed above, this paper deduces and establishes a more general large strain consolidation equation of sand-drained ground, which can consider factors that influence the large strain consolidation, such as the effect of resistance of sand well, the change in radial permeability coefficient and vertical seepage. The finite difference method is used to solve this equation, compare the difference with the existing consolidation model and the analytical solution of small deformation, and verify the accuracy of the solution. Based on the solution presented in this paper, the large strain consolidation behavior of sand-drained ground is analyzed.

2 Large strain consolidation equation of sand-drained ground

2.1 Calculation diagrams and coordinate system

Figure 1 is a simplified calculation diagram of the large strain consolidation of sand-drained ground, by considering effect of well resistance and change in radial permeability coefficient. q_p is the overburden load applied to the foundation soil surface before the load has been applied; q_u is the instantaneous load acting on the foundation soil surface; r_w, r_s and r_e are the radius of sand well, the radius of strong smear area and the radius of the affected area of sand well, respectively; $k_r = k_r(r)$ is the radial permeability coefficient of the soil in the sand well affected zone ($r_w \leqslant r \leqslant r_e$); k_v and k_w are the vertical permeability coefficients of the soil and the sand well, respectively; and G_s is the relative density of the soil particles. It is hypothesized that the upper boundary of sand-drained ground soil is the drainage boundary and that the lower boundary is not.

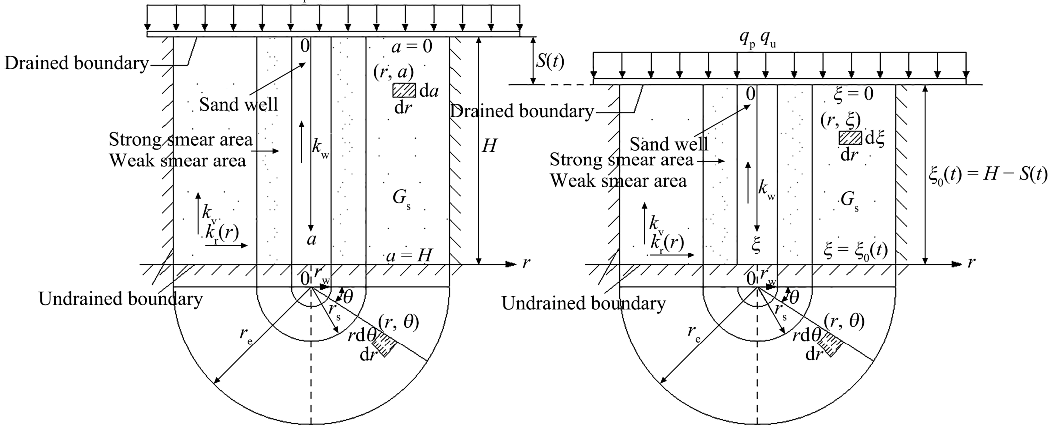

(a) Initial state (Lagrangian coordinate system) (b) Distribution at time *t* (Moving coordinate system)

Fig. 1 Calculation diagram of large strain consolidation of sand-drained ground

https://rocksoilmech.researchcommons.org/journal/vol42/iss3/5
DOI: 10.16285/j.rsm.2020.6029

Lagrange coordinate a or moving coordinate ξ is usually applied for establishing equations, as the upper boundary of soil will move down during the consolidation process of sand-drained ground. Fig. 1(a) shows the schematic diagram of the sand-drained ground in the Lagrangian coordinate system at the initial time. The initial thickness of the sand-drained ground is H and the top and bottom of the foundation are denoted as $a = 0$ and $a = H$, respectively. Fig. 1(b) presents the schematic diagram of the sand-drained ground in the moving coordinate system at time t. Let $S(t)$ be the amount of settlement on the surface of the sand-drained ground at time t, then the coordinates at the top and bottom of the sand-drained ground in the moving coordinate system could be recorded as $\xi = 0$ and $\xi = \xi_0(t) = H - S(t)$.

According to Gibson's one-dimensional large strain consolidation theory[22], the relationship of Lagrange coordinate a or moving coordinate ξ could be expressed as follows:

$$\frac{\partial \xi}{\partial a} = \frac{1+e}{1+e_0} \tag{1}$$

where $e = e(a, t)$, e is the void ratio of the soil; and $e_0 = e(a, 0)$, e_0 is the initial void ratio of the soil.

2.2 Basic hypotheses

Based on Barron's equal strain consolidation theory of sand-drained ground and Gibson's one-dimensional large strain consolidation theory, the following basic hypotheses could be made:

(a) The soil is fully saturated, soil particles and pore water are incompressible, and the foundation deformation is completely caused by the drainage of the pore water.

(b) The foundation soil only deforms vertically, does not move along the radial and tangential directions and does not consider the creep of soil.

(c) When the equal strain condition is established, the vertical deformation at each point of a same horizontal plane is the same within the sand well affected area.

(d) The seepage of water in soil follows the Darcy's law.

(e) The compressibility and permeability of soil vary non-linearly with the void ratio.

(f) The radial permeability coefficient $k_r(r)$ of the soil in the affected area of the sand well will change along the radial direction. By considering the effect of resistance of the sand well and that the permeability coefficient may gradually decrease due to several factors, such as the increase in lateral stress on the sand well, the fact that the entry of fine particles into the sand well may block the sand well and the vertical deformation of the sand well, as well as by taking references from relevant experimental studies conducted by Bo[23], Kim[24], Deng[25] and so on. It is hypothesized that the permeability coefficient k_w of sand well will decrease exponentially in coordination with the time needed for consolidation t:

$$k_w = k_{w0} \exp(-\omega t) \tag{2}$$

where k_{w0} is the initial permeability coefficient of the sand well and ω is a constant (1/s) greater than 0.

(7) The amount of water flowing into the sand well at any depth is equal to the increment of water flowing upward from the sand well.

2.3 Derivation of governing equations

Fig. 2 shows the vertical and radial seepages of soil units in the moving coordinate system.

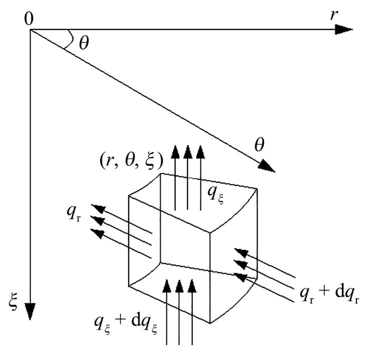

Fig. 2 Soil element in moving coordinate system

The amount of pore water flowing into and out of the vertical unit is respectively:

$$\left.\begin{aligned} & q_\xi = \frac{e}{1+e}(v_w^\xi - v_s)\cdot r\mathrm{d}\theta\mathrm{d}r \\ & q_\xi + \mathrm{d}q_\xi = \\ & \quad \left\{\frac{e}{1+e}(v_w^\xi - v_s) + \frac{\partial}{\partial \xi}\left[\frac{e}{1+e}(v_w^\xi - v_s)\right]\mathrm{d}\xi\right\}\cdot r\mathrm{d}\theta\mathrm{d}r \end{aligned}\right\} \tag{3}$$

where v_w^ξ and v_s are the actual velocities of pore water and soil particles, respectively along the vertical direction.

Therefore, the change in total vertical flow of the unit would be

$$\mathrm{d}q_\xi = \frac{\partial}{\partial \xi}\left[\frac{e}{1+e}(v_w^\xi - v_s)\right] r\mathrm{d}\theta\mathrm{d}r\mathrm{d}\xi \tag{4}$$

Since it is assumed that the horizontal and radial soil particles do not move, the amount of pore water flowing in and out of the radial direction are expressed respectively:

$$\left.\begin{aligned} &q_\mathrm{r}=\frac{e}{1+e}v_\mathrm{w}^\mathrm{r}\cdot r\mathrm{d}\theta\mathrm{d}\xi\\ &q_\mathrm{r}+\mathrm{d}q_\mathrm{r}=\\ &\quad\left[\frac{e}{1+e}v_\mathrm{w}^\mathrm{r}+\frac{\partial}{\partial r}\left(\frac{e}{1+e}v_\mathrm{w}^\mathrm{r}\right)\mathrm{d}r\right](r+\mathrm{d}r)\mathrm{d}\theta\mathrm{d}\xi \end{aligned}\right\} \tag{5}$$

where v_w^r is the actual velocity of pore water in radial direction. If the high-order term $\mathrm{d}r$ in Eq. (5) is omitted, the change in amount of radial pore water flow of the unit would be:

$$\mathrm{d}q_\mathrm{r}=\left[\frac{e}{1+e}v_\mathrm{w}^\mathrm{r}+\frac{\partial}{\partial r}\left(\frac{e}{1+e}v_\mathrm{w}^\mathrm{r}\right)r\right]\mathrm{d}\theta\mathrm{d}r\mathrm{d}\xi \tag{6}$$

The change in volume of the unit per unit time would be

$$\mathrm{d}V=-\frac{e}{1+e}\frac{\partial e}{\partial t}r\mathrm{d}\theta\mathrm{d}r\mathrm{d}\xi \tag{7}$$

According to the continuity condition of soil seepage consolidation, the change of unit volume in time $\mathrm{d}t$ is caused by the vertical and radial seepages of pore water, hence $\mathrm{d}V=\mathrm{d}q_\xi+\mathrm{d}q_\mathrm{r}$. By sorting out the Eqs. (4), (6) and (7), the following could be obtained:

$$\frac{e}{1+e}\frac{\partial e}{\partial t}+\frac{\partial}{\partial\xi}\left[\frac{e}{1+e}(v_\mathrm{w}^\xi-v_\mathrm{s})\right]+\left[\frac{e}{1+e}\frac{v_\mathrm{w}^\mathrm{r}}{r}+\frac{\partial}{\partial r}\left(\frac{e}{1+e}v_\mathrm{w}^\mathrm{r}\right)\right]=0 \tag{8}$$

The following could be obtained from the radial seepage that satisfies Darcy's law:

$$\frac{e}{1+e}v_\mathrm{w}^\mathrm{r}=-\frac{k_\mathrm{r}}{\gamma_\mathrm{w}}\frac{\partial u_\mathrm{s}}{\partial r} \tag{9}$$

where γ_w is the unit weight of water; and u_s is the excess pore pressure of soil at any point.

According to the hypothesis (3), the vertical strain of soil at a same depth is equal, therefore the regularity of the vertical seepage should correspond to the average excess pore pressure $\bar{u}_\mathrm{s}$ in soil at any depth. The following expression could be obtained from the vertical seepage that satisfies Darcy's law:

$$\frac{e}{1+e}(v_\mathrm{w}^\xi-v_\mathrm{s})=-\frac{k_\mathrm{v}}{\gamma_\mathrm{w}}\frac{\partial\bar{u}_\mathrm{s}}{\partial\xi} \tag{10}$$

where, the expression for $\bar{u}_\mathrm{s}$ is

$$\bar{u}_\mathrm{s}(\xi,t)=\frac{1}{\pi(r_\mathrm{e}^2-r_\mathrm{w}^2)}\int_{r_\mathrm{w}}^{r_\mathrm{e}}2\pi r\cdot u_\mathrm{s}(\xi,r,t)\mathrm{d}r \tag{11}$$

By sorting out Eqs. (8)–(10), the following equation could be obtained:

$$\frac{e}{1+e}\frac{\partial e}{\partial t}=\frac{k_\mathrm{r}}{\gamma_\mathrm{w}}\frac{1}{r}\frac{\partial u_\mathrm{s}}{\partial r}+\frac{1}{\gamma_\mathrm{w}}\frac{\partial}{\partial r}\left(k_\mathrm{r}\frac{\partial u_\mathrm{s}}{\partial r}\right)+\frac{\partial}{\partial\xi}\left(\frac{k_\mathrm{v}}{\gamma_\mathrm{w}}\frac{\partial\bar{u}_\mathrm{s}}{\partial\xi}\right) \tag{12}$$

According to the principle of effective stress of soil, this could be obtained:

$$\sigma'(\xi,t)=q_\mathrm{u}+\sigma_0'(\xi,t)-\bar{u}_\mathrm{s}(\xi,t) \tag{13}$$

where σ' is the vertical effective stress of soil; and σ_0' is the initial vertical effective stress of soil.

According to Eq. (13), the left term in Eq. (12) is transformed as follows:

$$\frac{1}{1+e}\frac{\partial e}{\partial t}=\frac{1}{1+e}\frac{\mathrm{d}e}{\mathrm{d}\sigma'}\frac{\partial\sigma'}{\partial t}=-\frac{1}{1+e}\frac{\mathrm{d}e}{\mathrm{d}\sigma'}\frac{\partial\bar{u}_\mathrm{s}}{\partial t} \tag{14}$$

By sorting out Eqs. (12) and (14), the following equation could be obtained:

$$\frac{1}{r}\frac{\partial}{\partial r}\left(r\frac{k_\mathrm{r}}{\gamma_\mathrm{w}}\frac{\partial u_\mathrm{s}}{\partial r}\right)=m_\mathrm{v}\frac{\partial\bar{u}_\mathrm{s}}{\partial t}-\frac{\partial}{\partial\xi}\left(\frac{k_\mathrm{v}}{\gamma_\mathrm{w}}\frac{\partial\bar{u}_\mathrm{s}}{\partial\xi}\right),\ r_\mathrm{w}\leqslant r\leqslant r_\mathrm{e} \tag{15}$$

$$m_\mathrm{v}=-\frac{1}{1+e}\frac{\mathrm{d}e}{\mathrm{d}\sigma'} \tag{16}$$

where m_v is the volumetric compression coefficient of soil. Eq. (15) is the governing equation of large strain consolidation of sand-drained ground.

The radial boundary conditions of the sand-drained ground are

$$\left.\frac{\partial u_\mathrm{s}}{\partial r}\right|_{r=r_\mathrm{e}}=0 \tag{17}$$

$$u_\mathrm{s}\big|_{r=r_\mathrm{w}}=u_\mathrm{w} \tag{18}$$

where u_w is the excess pore pressure in the sand well.

According to Appendix A, the expression for u_w is

$$u_\mathrm{w}=\frac{k_\mathrm{r}(r_\mathrm{w})(2\xi_0\xi-\xi^2)}{r_\mathrm{w}k_\mathrm{w}}\left(\left.\frac{\partial u_\mathrm{s}}{\partial r}\right|_{r=r_\mathrm{w}}\right) \tag{19}$$

To facilitate the derivation of the equation, let

$$\Gamma=m_\mathrm{v}\frac{\partial\bar{u}_\mathrm{s}}{\partial t}-\frac{\partial}{\partial\xi}\left(\frac{k_\mathrm{v}}{\gamma_\mathrm{w}}\frac{\partial\bar{u}_\mathrm{s}}{\partial\xi}\right) \tag{20}$$

By using the boundary conditions (17), the following equation could be obtained by integrating both sides of Eq. (15) with respect to r

$$\frac{\partial u_\mathrm{s}}{\partial r}=\frac{\gamma_\mathrm{w}}{2k_\mathrm{r}(r)}\Gamma\left(\frac{r^2-r_\mathrm{e}^2}{r}\right) \tag{21}$$

To consider the variation of the radial permeability coefficient k_r, let $k_\mathrm{r}(r)=k_\mathrm{h}f(r)$, where k_h is the radial permeability coefficient at the boundary $r=r_\mathrm{e}$ of the sand well's affected zone, and $f(r)$ is the function describing the variation of the permeability coefficient with respect to r.

Using Eq. (21) leads to

$$\left.\frac{\partial u_\mathrm{s}}{\partial r}\right|_{r=r_\mathrm{w}}=\frac{\gamma_\mathrm{w}r_\mathrm{w}(1-n^2)}{2k_\mathrm{h}f(r_\mathrm{w})}\Gamma \tag{22}$$

where $n = r_e / r_w$.

By using Eq. (22), Eq. (19) could be expressed as follows:

$$u_w = \frac{(2\xi_0 \xi - \xi^2)(1-n^2)\gamma_w}{2k_w}\Gamma \tag{23}$$

By using the boundary conditions Eq. (18), the following equation could be obtained by integrating both sides of Eq. (21) with respect to r:

$$u_s = -\frac{\gamma_w}{2k_h}\left[r_e^2 B_0(r) - C_0(r)\right]\Gamma + u_w \tag{24}$$

where $B_0(r) = \int_{r_w}^{r} \frac{1}{xf(x)}\mathrm{d}x$; $C_0(r) = \int_{r_w}^{r} \frac{x}{f(x)}\mathrm{d}x$.

Substituting Eq. (24) into Eq. (11), we have

$$\bar{u}_s = -\frac{\gamma_w r_e^2 R}{2k_h}\Gamma + u_w \tag{25}$$

$$R = \frac{2(r_e^2 B_1 - C_1)}{r_e^2 (r_e^2 - r_w^2)} \tag{26}$$

where $B_1 = \int_{r_w}^{r_e} rB_0(r)\mathrm{d}r$; $C_1 = \int_{r_w}^{r_e} rC_0(r)\mathrm{d}r$.

Substituting Eqs. (20), (23) into Eq. (25), we have

$$\bar{u}_s = -\left[\frac{\gamma_w r_e^2 R}{2k_h} + \frac{(2\xi_0\xi - \xi^2)(n^2-1)\gamma_w}{2k_w}\right]\cdot \left[m_v \frac{\partial \bar{u}_s}{\partial t} - \frac{\partial}{\partial \xi}\left(\frac{k_v}{\gamma_w}\frac{\partial \bar{u}_s}{\partial \xi}\right)\right] \tag{27}$$

The vertical boundary conditions of the sand-drained ground are:

$$\bar{u}_s\big|_{\xi=0} = 0 \tag{28}$$

$$\left.\frac{\partial \bar{u}_s}{\partial \xi}\right|_{\xi=\xi_0} = 0 \tag{29}$$

The initial condition for solving Eq. (27) is

$$\bar{u}_s\big|_{t=0} = q_u \tag{30}$$

Eq. (27) is the governing equation of large strain consolidation of sand-drained ground in the moving coordinate system. This equation is able to consider the effect of the factors including the effect of well resistance, the change in radial permeability coefficient and vertical seepage on large strain consolidation characteristic of sand well, therefore, it is more general. Eqs. (28)−(30) are conditions needed for the solving of the equation

3 Several modes of radial permeability coefficient's variation

In order to examine the effect of the change in radial permeability coefficient on the large strain consolidation behavior of sand-drained ground, this paper has considered 5 variation patterns of radial permeability coefficient of soil, as shown in Fig. 3, let $k_s = k_h f(r_w)$ and $\delta = f(r_w)$. In the first three variation patterns, it is hypothesized that the radial permeability coefficients are different in the strong smear area in coordination with r only and that it will remain constant in the weak smear area. In the latter two variation patterns, it is hypothesized that the radial permeability coefficient will vary in coordination with r in the whole affected area. In pattern 1, the radial permeability coefficient of strong smear area is considered to be a constant, as shown in Fig. 3(a). In pattern 2, it is hypothesized that the radial permeability coefficient of the strong smear area will increase linearly with r, as shown in Fig. 3(b). In pattern 3, it is hypothesized that the radial permeability coefficient of the strong smear area will change in a parabolic pattern as r increases, as shown in Fig. 3(c). In pattern 4, the radial permeability coefficient in the affected area is considered to be increased linearly with r, as shown in Fig. 3(d). In pattern 5, the radial permeability coefficient in the affected area is considered to be changed in a parabolic pattern as r increases, as shown in Fig. 3(e).

From the derivations above, it can be seen that the impact of soil radial permeability coefficient distribution is only related to the parameter R. For different variation patterns, the solution is the same except for the parameter R. The parameter R in these five patterns will be solved in the following passage.

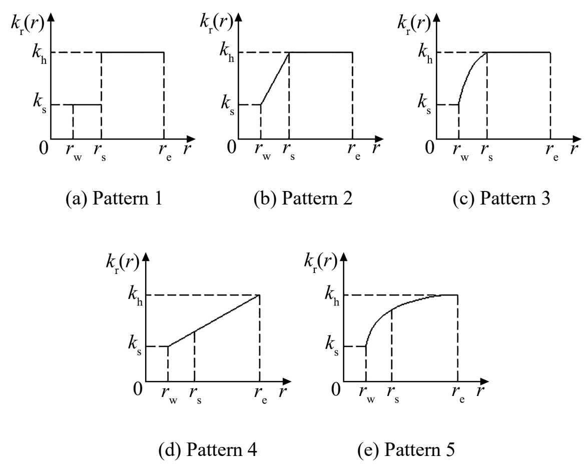

Fig. 3 Five variation patterns of radial permeability coefficient

3.1 Pattern 1

When the variation of radial permeability coefficient is in pattern 1, the following equation could be set according to Fig. 3(a):

$$f(r) = \begin{cases} \delta, & r_w \leqslant r \leqslant r_s \\ 1, & r_s < r \leqslant r_e \end{cases} \tag{31}$$

Substituting Eq. (31) into Eq. (26), we have

$$R=\frac{n^2}{n^2-1}\left(\ln\frac{n}{s}+\frac{1}{\delta}\ln s-\frac{3}{4}\right)+\frac{s^2}{n^2-1}\left(1-\frac{1}{\delta}\right)\left(1-\frac{s^2}{4n^2}\right)+\frac{1}{\delta(n^2-1)}\left(1-\frac{1}{4n^2}\right) \tag{32}$$

where $s=r_{\mathrm{s}}/r_{\mathrm{w}}$.

3.2 Pattern 2

When the variation of radial permeability coefficient is in pattern 2, the following equation could be set according to Fig. 3(b):

$$f(r)=\begin{cases}\dfrac{r-r_{\mathrm{w}}}{r_{\mathrm{s}}-r_{\mathrm{w}}}(1-\delta)+\delta,\ r_{\mathrm{w}}\leqslant r\leqslant r_{\mathrm{s}}\\ 1,\ r_{\mathrm{s}}<r\leqslant r_{\mathrm{e}}\end{cases} \tag{33}$$

Similarly, substituting Eq. (33) into Eq. (26) gives

$$R=\frac{n^2}{n^2-1}\left\{\frac{s-1}{\delta s-1}\ln(\delta s)-\frac{(s-1)^2}{n^2(1-\delta)}+\frac{2(s-1)(\delta s-1)}{n^2(1-\delta)^2}\cdot\ln\frac{1}{\delta}-\frac{2(s-1)}{n^4(1-\delta)}\left(\frac{s^3-1}{3}-\frac{s^2-1}{2}\right)-\frac{(s-1)(\delta s-1)}{n^4(1-\delta)^2}\cdot\left[\frac{s^2-1}{2}-\frac{(s-1)(\delta s-1)}{(1-\delta)}+\frac{(\delta s-1)^2}{(1-\delta)^2}\ln\frac{1}{\delta}\right]-\frac{(n^2-s^2)}{n^4}\frac{(1-s)^2}{(1-\delta)}+\ln\frac{n}{s}-\frac{3}{4}+\frac{4n^2s^2-s^4}{4n^4}\right\} \tag{34}$$

3.3 Pattern 3

When the variation of radial permeability coefficient is in pattern 3, the following equation could be set according to Fig. 3(c):

$$f(r)=\begin{cases}(1-\delta)\left(a-b+c\dfrac{r}{r_{\mathrm{w}}}\right)\left(a+b-c\dfrac{r}{r_{\mathrm{w}}}\right),\ r_{\mathrm{w}}\leqslant r\leqslant r_{\mathrm{s}}\\ 1,\ r_{\mathrm{s}}<r\leqslant r_{\mathrm{e}}\end{cases} \tag{35}$$

Here, $a=\sqrt{1/(1-\delta)}$; $b=s/(s-1)$; $c=1/(s-1)$.

Substituting Eq. (35) into Eq. (26) yields

$$R=\frac{a^2R_1+n^2R_2}{(n^2-1)} \tag{36}$$

where the expressions for R_1 and R_2 are

$$R_1=\frac{1}{a^2-b^2}\left(s^2\ln s-\frac{s^2}{2}+\frac{1}{2}\right)-\frac{1}{(a^2-b^2)c^2}\cdot\left[-b+\frac{1}{2}+\left(\frac{a^2}{2}-b^2\right)\ln\delta+\frac{abd}{2}\right]+\frac{1}{n^2c^4}\cdot\left[-3b+\frac{1}{2}+\left(\frac{a^2}{2}+b^2\right)\ln\delta+\frac{3abd}{2}\right] \tag{37}$$

$$R_2=\ln\frac{n}{s}-\frac{3}{4}+\frac{s^2}{n^2}-\frac{s^4}{4n^4}+a^2\left(1-\frac{s^2}{n^2}\right)\cdot\left[\frac{1}{(a^2-b^2)}\left(\ln(s\sqrt{\delta})-\frac{bd}{2a}\right)-\frac{1}{n^2c^2}\left(\ln\sqrt{\delta}+\frac{bd}{2a}\right)\right] \tag{38}$$

where $d=\ln\left[(a+1)/(a-1)\right]$。

3.4 Pattern 4

When the variation of radial permeability coefficient is in pattern 4, the following equation could be set according to Fig. 3(d):

$$f(r)=\frac{r-r_{\mathrm{w}}}{r_{\mathrm{e}}-r_{\mathrm{w}}}(1-\delta)+\delta,\ r_{\mathrm{w}}\leqslant r\leqslant r_{\mathrm{e}} \tag{39}$$

Substituting Eq. (39) into Eq. (26) results in

$$R=\frac{n^2}{n^2-1}\left\{\frac{n-1}{\delta n-1}\ln(\delta n)-\frac{(n-1)^2}{n^2(1-\delta)}+\frac{2(n-1)(\delta n-1)}{n^2(1-\delta)^2}\cdot\ln\frac{1}{\delta}-\frac{2(n-1)}{n^4(1-\delta)}\left(\frac{n^3-1}{3}-\frac{n^2-1}{2}\right)-\frac{(n-1)(\delta n-1)}{n^4(1-\delta)^2}\cdot\left[\frac{n^2-1}{2}-\frac{(n-1)(\delta n-1)}{(1-\delta)}+\frac{(\delta n-1)^2}{(1-\delta)^2}\ln\frac{1}{\delta}\right]\right\} \tag{40}$$

3.5 Pattern 5

When the variation of radial permeability coefficient is in pattern 5, the following equation could be set according to Fig. 3(e):

$$f(r)=1-(1-\delta)\left(\frac{r-r_{\mathrm{w}}}{r_{\mathrm{e}}-r_{\mathrm{w}}}\right)^2,\ r_{\mathrm{w}}\leqslant r\leqslant r_{\mathrm{e}} \tag{41}$$

Substituting Eq. (41) into Eq. (26), we have

$$R=D\ln n-\frac{E+F+D}{2}\left(1-\frac{1}{n^2}\right)+\frac{(AE-CF)}{B}\left(1-\frac{1}{n}\right)+E\left(1-\frac{A^2}{B^2}\right)\ln\left(\frac{n}{B+An}\right)+F\left(1-\frac{C^2}{B^2}\right)\ln\left(\frac{n}{Cn-B}\right) \tag{42}$$

where $A=1-\dfrac{n\sqrt{1-\delta}}{n-1}$; $B=1-A$; $C=2-A$; $D=\dfrac{1}{AC}$; $E=\dfrac{A}{2B^2}-\dfrac{1}{2A}$; $F=\dfrac{C}{2B^2}-\dfrac{1}{2C}$.

4 Solution of governing equations

In order to facilitate the solution of the equation, according to Eq. (1) and $\xi_0(t)=H-S(t)$, the governing Eq. (27) in the moving coordinate system can be firstly converted to the governing equation in the Lagrangian coordinate system, namely,

$$\bar{u}_{\mathrm{s}}=-\left(\frac{\gamma_{\mathrm{w}}r_{\mathrm{e}}^2R}{2k_{\mathrm{h}}}+\Lambda\right)\cdot\left[m_{\mathrm{v}}\frac{\partial\bar{u}_{\mathrm{s}}}{\partial t}-\frac{1+e_0}{1+e}\frac{\partial}{\partial a}\left(\frac{k_{\mathrm{v}}}{\gamma_{\mathrm{w}}}\frac{1+e_0}{1+e}\frac{\partial\bar{u}_{\mathrm{s}}}{\partial a}\right)\right] \tag{43}$$

$$\Lambda=\frac{(n^2-1)\gamma_{\mathrm{w}}}{2k_{\mathrm{w}}}\left\{2(H-S)\left[\int_0^a\frac{1+e(x,t)}{1+e(x,0)}\mathrm{d}x\right]-\left[\int_0^a\frac{1+e(x,t)}{1+e(x,0)}\mathrm{d}x\right]^2\right\} \tag{44}$$

To consider the changes in compressibility and permeability over void ratio during the large strain consolidation of sand-drained ground, the models $e-\lg\sigma'$ and $e-\lg k$ that have be widely used are adopted to describe the non-linear compression and permeability characteristics of soil[17−19]. Hence, the relationship between the void ratio of soil e and both the effective stress σ' and the permeability coefficient k could be expressed as follows:

$$\left.\begin{aligned}e&=e_{\mathrm{ref}}-C_{\mathrm{c}}\lg(\sigma'/\sigma'_{\mathrm{ref}})\\e&=e_{\mathrm{ref}}+C_{\mathrm{kh}}\lg(k_{\mathrm{h}}/k_{\mathrm{href}})\\e&=e_{\mathrm{ref}}+C_{\mathrm{kv}}\lg(k_{\mathrm{v}}/k_{\mathrm{vref}})\end{aligned}\right\} \tag{45}$$

where e_{ref} is the reference void ratio; σ'_{ref} , k_{href} and k_{vref} are respectively the corresponding effective stress, the radial permeability coefficient and the vertical permeability coefficient; C_{c} , C_{kh} and C_{kv} are respectively the compression index, the radial permeability index and the vertical permeability index of soil.

According to the relationships between non-linear compression and permeability listed above, the radial permeability coefficient and vertical permeability coefficient of soil could be written as follows:

$$\left.\begin{aligned}k_{\mathrm{h}}&=k_{\mathrm{href}}(\sigma'/\sigma'_{\mathrm{ref}})^{-C_{\mathrm{c}}/C_{\mathrm{kh}}}\\k_{\mathrm{v}}&=k_{\mathrm{vref}}(\sigma'/\sigma'_{\mathrm{ref}})^{-C_{\mathrm{c}}/C_{\mathrm{kv}}}\end{aligned}\right\} \tag{46}$$

According to Eq. (45), the volumetric compressibility coefficient of soil m_{v} could be obtained by using Eq. (16):

$$m_{\mathrm{v}}=\frac{C_{\mathrm{c}}}{(1+e)\sigma'\ln 10} \tag{47}$$

For large strain consolidation problem of sand-drained ground, it is usually difficult to obtain an analytical solution to the governing equation (43), as all of the radial permeability coefficient, vertical permeability coefficient and volumetric compressibility coefficient of soil vary significantly during the consolidation process. This paper intends to solve the governing equation (43) through finite difference method.

Let Δa and Δt be the space step and time step, respectively, then $a_i=i\Delta a$, i = 0, 1, 2, …, I, $t_j=j\Delta t$, j = 0, 1, 2, …, J. Therefore the implicit difference scheme of Eq. (43) could be written as

$$\bar{u}_{si}^{j+1}=-T_{ei}^{j}\frac{(\bar{u}_{si}^{j+1}-\bar{u}_{si}^{j})}{\Delta t}+\frac{H_{ei}^{j}}{\Delta a^2}\left[B_{\mathrm{v}i+1/2}^{j}(\bar{u}_{si+1}^{j+1}-\bar{u}_{si}^{j+1})+B_{\mathrm{v}i-1/2}^{j}(\bar{u}_{si-1}^{j+1}-\bar{u}_{si}^{j+1})\right] \tag{48}$$

By combining Eq. (2) with Eqs. (43)−(47), the expression for the corresponding coefficient in Eq. (48) could be written as

$$\left.\begin{aligned}
T_{ei}^{j}&=\left[\frac{\gamma_{\mathrm{w}}r_{\mathrm{e}}^2R}{2k_{\mathrm{href}}}\left(\frac{\sigma_i'^{j}}{\sigma'_{\mathrm{ref}}}\right)^{C_{\mathrm{c}}/C_{\mathrm{kh}}}+\Lambda_i^j\right]\cdot\frac{C_{\mathrm{c}}}{\sigma_i'^{j}(1+e_i^j)\ln 10}\\
\Lambda_i^j&=\frac{(n^2-1)\gamma_{\mathrm{w}}}{2k_{\mathrm{w0}}\exp(-\omega\cdot t_j)}\cdot\\
&\left[2(H-S^j)\left(\sum_{k=0}^{i}\frac{1+(e_k^j+e_{k-1}^j)/2}{1+(e_k^0+e_{k-1}^0)/2}\Delta a\right)-\left(\sum_{k=0}^{i}\frac{1+(e_k^j+e_{k-1}^j)/2}{1+(e_k^0+e_{k-1}^0)/2}\Delta a\right)^2\right]\\
H_{ei}^{j}&=\left[\frac{\gamma_{\mathrm{w}}r_{\mathrm{e}}^2R}{2k_{\mathrm{href}}}\left(\frac{\sigma_i'^{j}}{\sigma'_{\mathrm{ref}}}\right)^{C_{\mathrm{c}}/C_{\mathrm{kh}}}+\Lambda_i^j\right]\frac{1+e_i^0}{1+e_i^j}\\
B_{\mathrm{v}i\pm1/2}^{j}&=(B_{\mathrm{v}i}^{j}+B_{\mathrm{v}i\pm1}^{j})/2\\
B_{\mathrm{v}i}^{j}&=\frac{k_{\mathrm{vref}}}{\gamma_{\mathrm{w}}}\left(\frac{\sigma_i'^{j}}{\sigma'_{\mathrm{ref}}}\right)^{-C_{\mathrm{c}}/C_{\mathrm{kv}}}\frac{1+e_i^0}{1+e_i^j}\\
\sigma_i'^{j}&=q_{\mathrm{u}}+\sigma_i'^{0}-\bar{u}_{si}^{j}\\
S^j&=\sum_{i=1}^{I}\frac{(e_i^0+e_{i-1}^0)/2-(e_i^j+e_{i-1}^j)/2}{1+(e_i^0+e_{i-1}^0)/2}\Delta a\\
e_i^j&=e_{\mathrm{ref}}-C_{\mathrm{c}}\lg(\sigma_i'^{j}/\sigma'_{\mathrm{ref}})
\end{aligned}\right\} \tag{49}$$

The boundary conditions needed for solving the difference equation (48) are

$$\bar{u}_{s0}^{j}=0 \tag{50}$$

$$\bar{u}_{sI}^{j}=\bar{u}_{sI-1}^{j} \tag{51}$$

The initial condition needed is

$$\bar{u}_{i}^{0}=q_{\mathrm{u}} \tag{52}$$

For large strain consolidation of sand-drained ground, there are differences between consolidation degree in terms of settlement and the one in terms of pore pressure. The average pore pressure consolidation degree U_{p} of sand-drained ground can be expressed as follows:

$$U_{\mathrm{p}}=1-\frac{1}{q_{\mathrm{u}}}\sum_{i=1}^{I}\frac{1}{I}\left(\frac{\bar{u}_{si}^{j}+\bar{u}_{si-1}^{j}}{2}\right) \tag{53}$$

The ultimate amount of settlement could be expressed as follows:

$$S_{\mathrm{f}}=\sum_{i=1}^{I}\frac{(e_i^0+e_{i-1}^0)/2-(e_i^{\mathrm{f}}+e_{i-1}^{\mathrm{f}})/2}{1+(e_i^0+e_{i-1}^0)/2}\Delta a \tag{54}$$

where e_i^0 and e_i^{f} are the initial and final void ratios at node i, respectively.

By combining the Eq. (7) in Eq. (49) and Eq. (54), the average settlement consolidation degree U_s of sand-drained ground could be obtained and be expressed as follows:

$$U_s = S^j / S_f \quad (55)$$

The content listed above shows the finite difference solution of large strain consolidation of sand-drained ground based on the hypothesis of equal strain, considering the effect of well resistance and change in radial permeability coefficient. The calculation program SDLSCP01 is developed by using the finite difference solution above and it could be used to solve the large strain consolidation process of sand-drained ground.

5 Verification of the calculation program

5.1 Comparison with the ALSC model

In order to verify the accuracy of the solution presented in this paper, it is compared to the ALSC model established by Cao et al.[16] by assuming that the permeability coefficient of sand well $k_{w0} = 10^{10} k_{href}$, $\omega = 0$ (ignoring the effect of well resistance) and the variation pattern of radial permeability coefficient is in pattern 1. By considering that the consolidation of sand-drained ground has been completed under overburden load q_p and the effect of weight, the calculation parameters of sand-drained ground could be presented as shown in Table 1.

Table 1 Calculation parameters of the sand-drained ground

Thickness H /m	e_{ref}	k_{href} /(m • s^{-1})	k_{vref} /(m • s^{-1})	σ'_{ref} /kPa	δ	q_u /kPa	q_p /kPa	G_s	C_c	C_{kh}	C_{kv}	r /m		
												r_e	r_s	r_w
10	3.0	4×10^{-8}	3.2×10^{-8}	10	0.2	100	10	2.7	1.0	0.8	0.8	0.7	0.28	0.07

Figure 4 describes the comparison between the calculation results using the finite difference solution presented in this paper and those from the ALSC model. It can be seen from the comparison of results in Fig. 4 that the finite difference solution is fully consistent with the variation pattern of the consolidation degree and the distribution pattern of average excess pore pressure along the depth obtained by the ALSC model by Cao et al.[16]. This suggests that the calculation program could be used to solve the consolidation problem of sand-drained ground and that the finite difference solution obtained in this paper is correct.

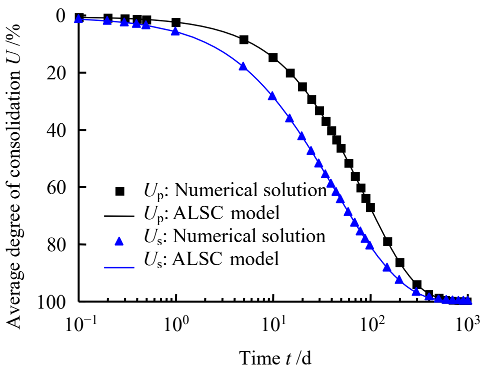

(a) Average degree of consolidation

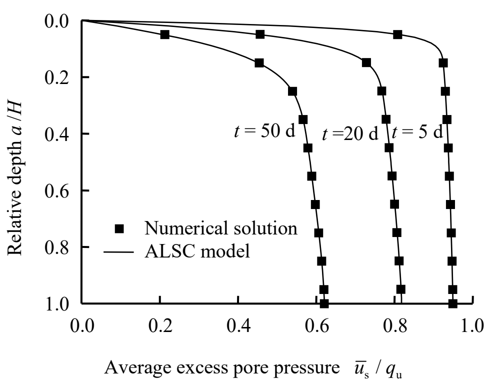

(b) Average excess pore pressure

Fig. 4 Comparison between the numerical solution and ALSC model

5.2 Comparison with the analytical solutions of small deformation

In order to verify the accuracy of the solution further, the numerical solution presented in this paper can be compared with the analytical solution under the hypothesis of small deformation proposed by Tang et al.[26]. The calculation parameters of sand-drained ground are set as follows: r_w = 0.04 m; s = 4; n = 12; H = 10 m; k_{w0} = 1.0 × 10^{-4} m/s; e_0 = 2.5; e_{ref} = 2.5; k_{href} = 2.0×10^{-8} m/s; k_{vref} = 1.5 × 10^{-8} m/s; σ'_{ref} = 20 kPa; δ = 0.2; C_c = 0.8; C_{kh} = C_{kv} = 0.6. Additionally, it is assumed that the variation pattern of radial permeability coefficient is in pattern 1. Meanwhile, since the change in sand permeability coefficient over time was not considered in the analytical solution of Tang et al.[26], it is assumed that $\omega = 0$. When the external load is small, the compressibility and permeability of the soil in the consolidation process can be considered as almost constant, therefore the external loads applied here are assumed to be q_u = 1.0, 5.0 and 20 kPa. During the comparison of calculations, the values of relevant parameters for foundation are different. When the analytical solution of small deformation is used for calculation, the initial values of the relevant parameters of foundation should be taken for calculation, and they will remain constant during the consolidation process; when the numerical solutions presented in this paper are used for calculation, the change in relevant foundation parameters during the consolidation process should be considered.

Figure 5 presents the comparison between the two solutions for calculating the average pore pressure consolidation degree U_p of sand-drained ground. As what can be seen from Fig. 5, when the external load is small, the curve of the average pore pressure consolidation degree obtained by the numerical solution has nearly superposed to the one obtained by the analytical solution of small deformation. Meanwhile, the smaller the external load is, the smaller the difference between the curves of the average pore pressure consolidation degree under these two solutions will be, and this has further verified the accuracy of the numerical solutions in this paper.

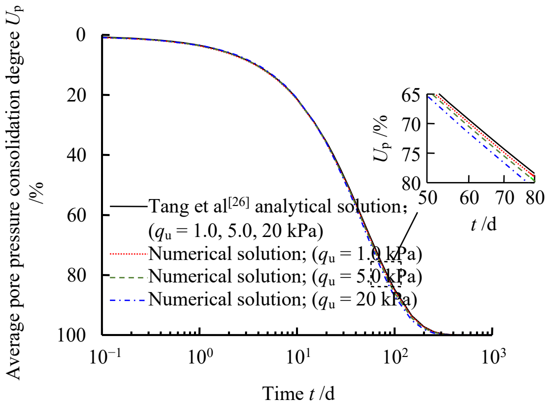

Fig. 5 Comparison between the numerical solution and Tang et al's analytical solution[26]

6 Analysis of consolidation behavior

In order to study the consolidation behavior of sand-drained ground with large deformation under changes in well resistance and radial permeability coefficient, several factors affecting the consolidation behavior of sand-drained ground will be analyzed based on the finite difference solution shown above. Factors include the k_{w0}/k_{href}, the variation pattern of radial permeability coefficient, the vertical seepage, the C_c/C_{kh} and C_c/C_{kv}. Here, the calculated parameters of sand-drained ground in Table 1 are taken as the reference and the variation pattern of radial permeability coefficient is set as in pattern 5, $k_{w0} = 2 \times 10^3$ k_{href}, $\omega = 1.6 \times 10^{-7}$ s^{-1}.

Figure 6 illustrates the variation of the average pore pressure degree U_p of sand-drained ground over time under different values of k_{w0}/k_{href}. It can be seen that the effect of resistance of sand well will reduce the consolidation rate of sand-drained ground as well as that the foundation consolidation rate will increase as the k_{w0}/k_{href} increases. Additionally, as the permeability of sand well decreases over time for consolidation, the effect of well resistance on the consolidation rate is shown to be more and more significant, especially when the k_{w0}/k_{href} is small. However, according to the consolidation curves of average pore pressure degree under different values of k_{w0}/k_{href}, the consolidation rate of sand-drained ground is increased significantly in coordination with increasing permeability coefficient of sand well when the value k_{w0}/k_{href} is less than 5 000. When the k_{w0}/k_{href} is greater than 5 000, the change of permeability coefficient of sand well has slight effect only on the consolidation rate of sand-drained ground. Therefore, from the perspective of engineering practice, the effect of well resistance of sand-drained ground could be ignored when the k_{w0}/k_{href} surpasses 5 000.

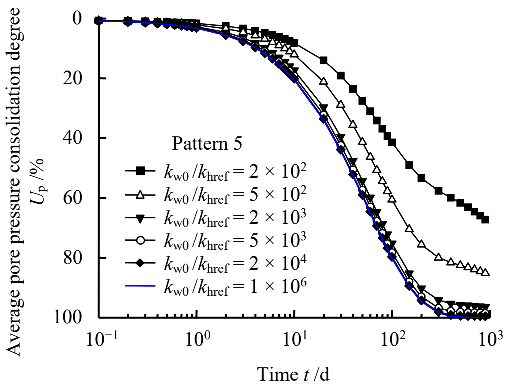

Fig. 6 Influence of k_{w0}/k_{href} on the average pore pressure consolidation degree

Figure 7 shows the change in average pore pressure degree U_p of sand-drained ground over time under different variation patterns of radial permeability coefficient. As what could be seen from the figure, when the radial permeability coefficient varies with r in the strong smear area only (patterns 1−3), the consolidation rate is the fastest in the parabolic pattern of radial permeability coefficient, then in the linear pattern and slowest in the constant pattern. When the radial permeability coefficient varies with r in the affected zone (patterns 4−5), the consolidation rate in the parabolic variation pattern is faster than the one in the linear variation pattern. By comparing these five radial permeability coefficient variation patterns, it can be seen that different radial permeability coefficient variation patterns would cause a great influence on the consolidation rate of sand-drained ground. The consolidation rate of pattern 1 is the slowest, whilst the one of pattern 3 is the fastest. By comparing them to the linear variation pattern, the consolidation rate of parabolic variation pattern is relatively faster.

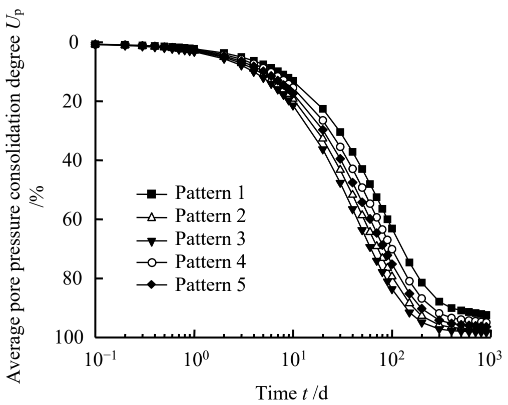

Fig. 7 Influence of the variation patterns of radial permeability coefficient on the average pore pressure consolidation degree

To ascertain the influence of vertical seepage on the consolidation rate of sand-drained ground, Fig. 8 presents the change in average pore pressure consolidation degree of sand-drained ground U_p over time for different H/r_e and k_{vref}/k_{href}. From Fig. 8, we can see that the vertical seepage has accelerated the consolidation rate of sand-drained ground. The greater the k_{vref}/k_{href} is, the greater the influence of vertical seepage on the consolidation rate of sand-drained ground will be; the smaller the H/r_e is, the greater the influence of vertical seepage on sand-drained ground will be. It can be seen from the consolidation curves of sand-drained ground under different H/r_e and k_{vref}/k_{href} values that when H/r_e is small (e.g. H/r_e < 7.14), the influence of vertical seepage on the consolidation of sand-drained ground should be considered.

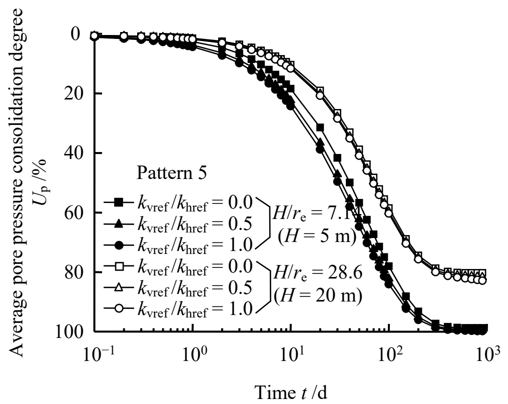

Fig. 8 Influence of vertical flow on the average pore pressure consolidation degree under different H/r_e and k_{vref}/k_{href}

Berry et al.[27]'s study has pointed out that the ratio of compression index to permeability index was mostly between 0.5 and 2.0. In the following analysis, The C_c/C_{kh} and C_c/C_{kv} are all taken in this range. Figs. 9 and 10 respectively show the average pore pressure consolidation degree curves of sand-drained ground with different C_c/C_{kh} and C_c/C_{kv} values. It can be seen from Fig. 9 that the C_c/C_{kh} has a significant effect on the consolidation rate of sand-drained ground. At a same time, the larger the C_c/C_{kh} is, the smaller the average pore pressure consolidation degree is. It can be observed from Fig. 10 that the consolidation rate of sand-drained ground will slow as the C_c/C_{kv} increases, but the change in C_c/C_{kv} has only slight effect on the consolidation rate. As what could be seen from Figs. 9 and 10, a greater ratio of compression index to permeability index leads to a slower consolidation rate. However, due to the short path of the radial seepage, the radial seepage is the main factor that controls the consolidation rate of sand-drained ground, therefore the C_c/C_{kh} has a great impact on the consolidation rate of sand-drained ground.

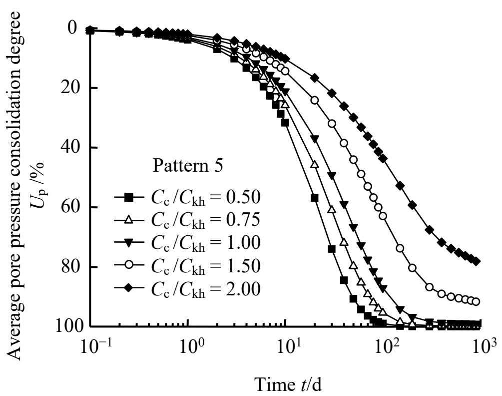

Fig. 9 Influence of C_c/C_{kh} on the average pore pressure consolidation degree

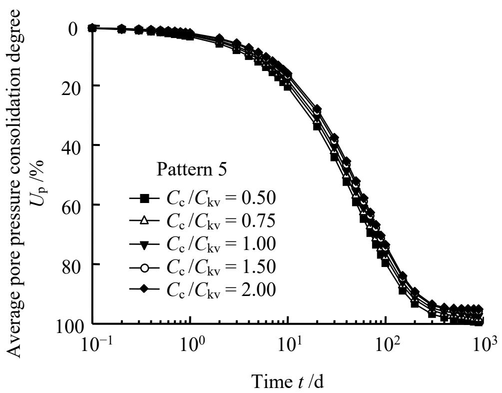

Fig. 10 Influence of C_c/C_{kv} on the average pore pressure consolidation degree

7 Conclusion

Through above study, conclusions can be drawn as follows:

(1) The resistance of sand well reduces the consolidation rate of sand-drained ground. However, from the

perspective of engineering practice, the effect of resistance of sand well on the consolidation rate could be ignored when the value of k_{w0}/k_{href} is greater than 5 000.

(2) The mode of radial permeability coefficient has a great impact on the consolidation rate of sand-drained ground. The consolidation rate is faster in the parabolic mode compared to linear mode. In this study, mode 1 has the slowest consolidation rate and mode 3 has the fastest consolidation rate.

(3) Vertical seepage accelerates the consolidation rate of sand-drained ground. When the H/r_e is relatively small (e.g. H/r_e less than 7.14), the effect of vertical seepage on the consolidation rate of sand-drained ground should be considered.

(4) The greater the ratio of compression index to permeability index is, the slower the consolidation rate of sand-drained ground will be. As radial seepage is the main factor that controls the consolidation rate of sand-drained ground, C_c/C_{kh} will have a significant impact on the consolidation rate of sand-drained ground.

References

[1] INDRARATNA B. Recent advances in the application of vertical drains and vacuum preloading in soft soil stabilization[J]. Australian Geomechanics Society, 2010, 45(2): 1−43.

[2] BARRON R A. Consolidation of fine-grained soils by drain wells[J]. Transactions of American Society of Civil Engineers, 1948, 74(6): 718−742.

[3] HANSBO S, JAMIOLKOWSKI M, KOK L. Consolidation by vertical drains[J]. Géotechnique, 1981, 31(1): 45−66.

[4] XIE Kang-he, ZENG Guo-xi. Consolidation theories for drain walls under equal strain condition[J]. Chinese Journal of Geotechnical Engineering, 1989, 11(2): 3−17.

[5] HANSBO S. Aspects of vertical drain design: Darcian or non-Darcian flow[J]. Géotechnique, 1997, 47(5): 983−992.

[6] TANG X W, ONITSUKA K. Consolidation of double-layered ground with vertical drains[J]. International Journal for Numerical and Analytical Methods in Geomechanics, 2001, 25(14): 1449−1465.

[7] INDRARATNA B, RUJIKIATKAMJORN C, SATHANANTHAN L. Analytical and numerical solutions for a single vertical drain including the effects of vacuum preloading[J]. Canadian Geotechnical Journal, 2005, 42(4): 994−1014.

[8] DENG Y B, XIE K H, LU M M, et al. Consolidation by prefabricated vertical drains considering the time dependent well resistance[J]. Geotextiles and Geomembranes, 2013, 36(1): 20−26.

[9] LU M, WANG S, SLOAN S W, et al. Nonlinear consolidation of vertical drains with coupled radial–vertical flow considering well resistance[J]. Geotextiles and Geomembranes, 2015, 43(2): 182−189.

[10] GUO Xiao, XIE Kang-he, LU Meng-meng et al. Nonlinear analytical solution for consolidation of vertical drains by straight-line vacuum preloading method[J]. Journal of Central South University (Science and Technology), 2018, 49(2): 384−392.

[11] ZHANG Yu-guo, WAN Dong-yang, ZHENG Yan-lin, et al. Analytical solution for consolidation of vertical drain under vacuum preloading considering the variation of radial permeability coefficient[J]. Rock and Soil Mechanics, 2019, 40(9): 3533−3541.

[12] JIANG Hui-huang, ZHAO You-ming, LIU Guo-nan, et al. Large strain consolidation of soft ground with vertical drains[J]. Chinese Journal of Geotechnical Engineering, 2011, 33(2): 302−308.

[13] ZHANG Ming, WANG Wei, LIU Qi-xia, et al. Consolidation behaviors of double-layered vertical drains ground considering power function permeability and compressibility variation[J]. Rock and Soil Mechanics, 2013, 34(11): 3117−3126.

[14] SUN Li-qiang, JIA Tian-qiang, YAN Shu-wang, et al. Study on consolidation theory of foundation with partially penetrated sand wells based on large strain[J]. Chinese Journal of Rock Mechanics and Engineering, 2017, 36(2): 248−256.

[15] CAO Yu-peng, SUN Zong-jun, DING Jian-wen, et al. Axisymmetric large-strain consolidation model for dredged clay with high water content[J]. Chinese Journal of Geotechnical Engineering, 2016, 38(10): 1904−1910.

[16] CAO Y, YANG J, XU G, et al. Analysis of large-strain consolidation behavior of soil with high water content in consideration of self-weight[J]. Advances in Civil Engineering, 2018, 2018(6): 1−10.

[17] INDRARATNA B, ZHONG R, FOX J, et al. Large-strain vacuum-assisted consolidation with non-Darcian radial flow incorporating varying permeability and compressibility[J]. Journal of Geotechnical and Geoenvironmental Engineering, 2016, 143(1): 04016088.

[18] GENG X, YU H S. A large-strain radial consolidation theory for soft clays improved by vertical drains[J]. Géotechnique, 2017, 67(11): 1−9.

[19] NGUYEN B P, KIM Y T. Radial consolidation of PVD-Installed normally consolidated soil with discharge capacity reduction using large-strain theory[J]. Geotextiles and

Geomembranes, 2019, 47(2): 243−254.

[20] GUO Biao, GONG Xiao-nan, LU Meng-meng, et al. Theoretical analysis on partially penetrated and drains foundation with consideration on smear effect[J]. Chinese Journal of Rock Mechanics and Engineering, 2009, 28(12): 2561−2568.

[21] GUO Biao, GONG Xiao-nan, LU Meng-meng, et al. Analytical solution for consolidation of vertical drains by vacuum-surcharge preloading[J]. Chinese Journal of Geotechnical Engineering, 2013, 35(6): 1045−1054.

[22] GIBSON R E, ENGLAND G L, HUSSEY M J. The theory of one-dimensional soil consolidation of saturated clays, I. finite nonlinear consolidation of thin homogeneous layers[J]. Géotechnique, 1967, 17(3): 261−273.

[23] BO M W. Discharge capacity of prefabricated vertical drain and their field measurements[J]. Geotextiles and Geomembranes, 2004, 22(1): 37−48.

[24] KIM R, HONG S J, LEE M J, et al. Time dependent well resistance factor of PVD[J]. Marine Georesources and Geotechnology, 2011, 29(2): 131−144.

[25] DENG Y B, LIU G B, LU M M, et al. Consolidation behavior of soft deposits considering the variation of prefabricated vertical drain discharge capacity[J]. Computers and Geotechnics, 2014, 30(8): 310−316.

[26] TANG X W, ONITSUKA K. Consolidation by vertical drains under time-dependent loading[J]. International Journal for Numerical and Analytical Methods in Geomechanics, 2000, 24(9): 739−751.

[27] BERRY P L, WILKINSON W B. The radial consolidation of clay soils[J]. Géotechnique, 1969, 19(2): 253−284.

Appendix A: Derivation of the excess pore pressure u_{w} in sand well

Figure A1 is a schematic diagram describing the flow of pore water from the soil around the well into the sand well. It is assumed here, that the flow rate of pore water from the soil at any depth around the well into the sand well is the same[19], hence the discharge of water flow $Q_{\mathrm{v}\xi}(t)$ at depth ξ could be written as

$$Q_{\mathrm{v}\xi}(t)=\frac{Q_{\mathrm{in}}(t)}{\xi_0}(\xi_0-\xi) \tag{A1}$$

where $Q_{\mathrm{in}}(t)$ is the total discharge of water flow from pore in the soil around the well into the sand well at time *t*.

According to the seepage rule of water in sand well, the water flow $Q_{\mathrm{v}\xi}(t)$ at depth ξ of the sand well could also be written as

$$Q_{\mathrm{v}\xi}(t)=\pi r_{\mathrm{w}}^2\frac{k_{\mathrm{w}}}{\gamma_{\mathrm{w}}}\frac{\partial u_{\mathrm{w}}}{\partial \xi} \tag{A2}$$

where u_{w} represents the excess pore pressure in the sand well and $u_{\mathrm{w}}=u_{\mathrm{w}}(\xi,t)$.

At any time *t*, by combining with Eq. (A1), expanding both sides of Eq. (A2) and integrating ξ, we have

$$\int_0^{\xi}Q_{\mathrm{in}}(t)\frac{(\xi_0-\xi)}{\xi_0}\mathrm{d}\xi=\int_0^{\xi}\frac{k_{\mathrm{w}}}{\gamma_{\mathrm{w}}}\pi r_{\mathrm{w}}^2\mathrm{d}u_{\mathrm{w}} \tag{A3}$$

Since the upper boundary of the sand well is the drainage boundary, the upper boundary condition $u_{\mathrm{w}}\big|_{\xi=0}=0$ could be used to carry out the integral of Eq. (A3):

$$Q_{\mathrm{in}}(t)\frac{(2\xi_0\xi-\xi^2)}{2\xi_0}=\frac{k_{\mathrm{w}}}{\gamma_{\mathrm{w}}}\pi r_{\mathrm{w}}^2u_{\mathrm{w}} \tag{A4}$$

The following equation could be obtained using Eq. (A4):

$$u_{\mathrm{w}}=\frac{(2\xi_0\xi-\xi^2)\gamma_{\mathrm{w}}Q_{\mathrm{in}}(t)}{2\pi r_{\mathrm{w}}^2\xi_0k_{\mathrm{w}}} \tag{A5}$$

At any time *t*, the total flow discharge $Q_{\mathrm{in}}(t)$ of pore water in the soil around the well into the sand well could be written as

$$Q_{\mathrm{in}}(t)=2\pi r_{\mathrm{w}}\xi_0\frac{k_{\mathrm{r}}(r_{\mathrm{w}})}{\gamma_{\mathrm{w}}}\left(\frac{\partial u_{\mathrm{s}}}{\partial r}\bigg|_{r=r_{\mathrm{w}}}\right) \tag{A6}$$

Therefore, by substituting Eq. (A6) into Eq. (A5), the expression of excess pore pressure u_{w} in sand well could be given as

$$u_{\mathrm{w}}=\frac{k_{\mathrm{r}}(r_{\mathrm{w}})(2\xi_0\xi-\xi^2)}{r_{\mathrm{w}}k_{\mathrm{w}}}\left(\frac{\partial u_{\mathrm{s}}}{\partial r}\bigg|_{r=r_{\mathrm{w}}}\right) \tag{A7}$$

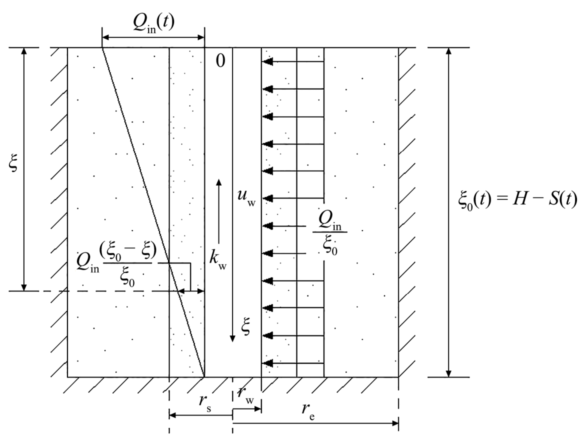

Fig. A1 Schematic diagram of water balance of the drain in convective coordinate syste